Materials Today Communications 40 (2024) 109441

Contents lists available at ScienceDirect

Materials Today Communications

journal homepage: www.elsevier.com/locate/mtcomm

Tunable dye adsorbing materials from crab and shrimp waste shells for water remediation

C. Triunfo [a,b], K. Tsirtsidou [c,d], K. Vanhoutte [c], A. Mucaria [a], D. Montroni [a], S. Fermani [a], G. Falini [a,*], J. Robbens [c]

[a] Department of Chemistry "Giacomo Ciamician", University of Bologna, via F. Selmi 2, Bologna 40126, Italy
[b] Fano Marine Center, Viale Adriatico 1/N 61032, Fano, Italy
[c] Aquatic Environment and Quality, Cell Blue Biotech and Food Integrity, Flanders Research Institute for Agriculture, Fisheries and Food (ILVO), Jacobsenstraat 1, Ostend 8400, Belgium
[d] Research Unit VEG-i-TEC, Department of Food Technology, Safety and Health, Ghent University Campus, Sint-Martens-Latemlaan 2B, Kortrijk 8500, Belgium

ARTICLE INFO

Keywords:
Water remediation
Organic dyes
Waste shells
Chitin
Calcium carbonate

ABSTRACT

Crab and shrimp shells are waste byproducts from shellfish farming and processing. In this study, we demonstrated that it is possible to obtain individual shell components either separately or in combinations. These diverse materials were composed of calcium carbonate and organic molecules inter- and intra-mineral, calcium carbonate and organic molecules intra-mineral, organic molecules such as chitin and proteins, only calcium carbonate, and only chitin. These substrates were tested for the adsorption of Methylene Blue and Eosin dyes. The goal is to demonstrate that the organic dye adsorption capacity can be modified by controlling the degree of deconstruction of the starting material. The best adsorption for the positively charged Methylene Blue was achieved on the chitin-calcium carbonate substrates, while the negatively charged Eosin adsorbed best on the chitin substrate. In conclusion, this research demonstrates that it is possible to obtain different materials by deconstructing the shells from crabs and shrimps at various levels reducing the generation of additional wastes. Moreover, these materials exhibit features that are related to the original material and possess new properties that can be also exploited in other fields like material sciences.

1. Introduction

Shellfish cultivation is an expanding economic activity worldwide. Moreover, in recent years, people's awareness of marine resources has improved. Shells are often considered as waste, despite their potential valorization as a residual side-stream, and therefore waste shells have aroused great concern. Every year, close to 8 million tons of waste crab, shrimp, and lobster shells are produced globally [1]. Since only about 40 wt% of the total weight of these crustaceans is edible, the crustacean farming and processing industry will produce a large quantity of waste shells [2]. However, due to the constraints associated to an integrated utilization technology and to unregulate disposal procedures, a large amount of shells are directly discarded or deposited as waste with a wide and complex distribution [3]. Shell piles and burials are common near beaches and seafood processing plants. Thereafter, they modify soils, waters, and marine ecosystems, particularly if their disposal is uncontrolled [4,5]. Moreover, they cause environmental damage by decomposition, emanating foul odors, as well as adding to visual pollution [6].

From the perspective of resource utilization, crustacean shells, such as those from crabs and shrimps, are rich in α-chitin, proteins and calcium carbonate ($CaCO_3$) [7]. It is well known that chitin and its derivatives are widely used in the pharmaceutical [8], cosmetic [9], environment and energy industry [10]. $CaCO_3$ is extensively used in the pharmaceutical, agricultural, construction, chemical, and polymer industry [11].

Current processes for crab and shrimp waste shells utilization focus on the extraction of chitin, chitosan [12] or bioactive compounds [13] often via sustainable and environmentally friendly synthetic extraction approaches. Moreover, the other residual shell materials are mostly discarded, even if they possess potential value [14].

A processing strategy in which all the components of the waste shell are recovered is desirable. A top down approach has been used to produce calcium carbonate-enriched chitosan from shrimp shell wastes to

* Corresponding author.
E-mail address: giuseppe.falini@unibo.it (G. Falini).

https://doi.org/10.1016/j.mtcomm.2024.109441
Received 23 January 2024; Received in revised form 14 May 2024; Accepted 2 June 2024
Available online 3 June 2024

valorize $CaCO_3$ [15]. Recycling shell waste could potentially eliminate the disposal problem and could also turn an otherwise useless waste into high value–added products. A cascading approach in which compounds of highest value are initially extracted, after which the residual biomass can be used for low end application, can even lead to zero-waste.

Here, we applied chemical and thermal processes that allowed to extract singularly or combined the main different components of crustacean waste shells. We characterized them for their chemical and physical features and as proof of concept for their valorisation/utilisation we used them as adsorbent of dyes from model polluted waters.

Materials derived from crustacean waste shells have already largely been used for the removal of contaminants from industrial effluents such as heavy metals [16–18], anionic pollutants [19,20], nitrogen [21] and dyes [22–24] but in our study, we are able to design new structures composed from shell material but with different properties.

Crab shell and chitosan powder were used to trap water-soluble dyes present in textile dyeing wastewater [25]. Low molecular weight (20 kDa) crab shell chitosan can also significantly reduce chemical oxygen demand, total suspended solids, total dissolved solids, and turbidity in textile mill wastewater [26]. Dai et al. used calcium-rich biochar obtained from crab shell to adsorb the cationic malachite green (12.5 mg g^{-1}) and the anionic Congo red (20.3 mg g^{-1}) dye but in this case a pyrolysis process was necessary to obtain the adsorbent [27]. Chitosan derived from shrimp shells (or peels) was applied as potential bio-adsorbent for Methyl Orange (MO) dye removal from waste water with the maximum adsorption capability of 0.1297 mg g^{-1} [28]. For $CaCO_3$, that is -next to chitin- the other main fraction of the residual shell, single crystals of calcite and aragonite were used to adsorb organic dyes. It was shown that aragonite and calcite have selective adsorption capability [29].

At present, crab and shrimp shell waste is primarily utilized for chitin extraction following an acid treatment to eliminate calcium carbonate and an alkaline treatment to eliminate the protein content and partially convert chitin to chitosan. The extraction of calcium carbonate from crab and shrimp shells, as well as its composites with organic molecules from the original material, has not been previously explored. The method described in this study is a new development in this area.

Since each singular component of crustacean shells has a specific adsorption capability, in this research we explore the hypothesis that newly developed material, consisting of multi-component extract can have an adsorption capability that is increased by the synergic action of the single components. To prove this hypothesis the waste shells from the market relevant species Brown Shrimp (BS) *Crangon crangon* and the invasive Chinese Mitten Crab (CMC) *Eriocheir sinensis* were used. They were differently chemically thermally treated and the obtained materials were tested for the adsorption of acidic and basic dyes relevant in the fabric industries.

2. Materials and methods

Reagents and solvents were purchased from Sigma Aldrich. All the chemicals were of analytical purity and were used without any purification process. For each experiment, daily fresh solutions were prepared. The waste shells from Brown Shrimp (*Crangon crangon*) and Chinese Mitten Crab (*Eriocheir sinensis*) were obtained from providers in Nieuwpoort and Grobbendonk (Belgium), respectively, in the form of powders. No information has been provided about the process by which they were produced. The shells fragments were washed with tap water and dried in an oven overnight at 50 °C.

2.1. Deproteinization reaction

A typical reflux setup was used for the deproteinization reaction where 1 g of each sample was put in a round bottom flask together with 40 mL of a 1 M NaOH solution freshly prepared. The NaOH solution was changed every hour and the total reaction time was 4 h for the shrimp and 5 h for the crab shells. The resultant suspensions were filtered and the fragments were washed with deionized water until the pH was close to neutral (about 6.5), then the samples were dried in an oven overnight at 60 °C.

2.2. Bleaching reaction

One g of each sample was put in a beaker (100 mL) together with 50 mL of a 5 % v/v NaClO solution and stirred on a rocking table for 8 days. The NaClO solution was changed every day. The resultant suspensions were filtered and the fragments were first washed with deionized water and then dried under vacuum in a desiccator overnight.

2.3. Thermal treatment

A certain amount of the bleached material, usually 0.3 g, from each species was thermally treated in an oven at 220 °C for 48 h in air environment.

2.4. Chitin extraction

In order to extract chitin from the starting material of each species, two steps were needed, i. e. a demineralization and a deproteinization process. The first one was performed suspending the waste shells (1 g) in a 1.5 M HCl solution (10 mL) for the shrimp and 2 M (25 mL) for the crab under magnetic bar stirring at 500 rpm. The reaction time was 2.5 h for the shrimp and 3 h for the crab. The resultant suspensions were filtered and the fragments were washed with deionized water until the pH was close to neutral (about 6.5), and dried in an oven overnight at 65 °C. The obtained fragments were, then, subjected to a deproteinization reaction. One g of fragments was suspended in a 1 M NaOH solution (10 mL for the shrimp and 25 mL for the crab) under magnetic stirring at 500 rpm. The reaction time and the experimental temperature were 2 h and 80 °C for the shrimp and 3 h and 90 °C for the crab, respectively. The resultant suspensions were filtered and the fragments were washed with deionized water until the pH was close to neutral, then the samples were dried in an oven overnight at 60 °C.

2.5. X-ray powder diffraction analysis

X-ray powder diffraction patterns were collected using a Pan-Analytical X'Pert Pro diffractometer equipped with a multi-array X'Celerator detector (PanAnalytical Instruments) using Cu Kα radiation ($\lambda = 1.54056$ Å) generated at 40 kV and 40 mA. The diffraction patterns were collected in the 2θ range between 5 ° and 60 ° with a step size (Δ2θ) of 0.05 ° and a counting time of 60 s. Each sample was ground with mortar and pestle before the measurement.

2.6. Fourier transform spectroscopic analysis

A Thermo Scientific™ Nicolet™ iS™10 FTIR Spectrometer was used to collect the FTIR spectra. Disk sample for FTIR analysis was obtained by mixing a small amount (2 mg) of product with 100 mg of KBr and applying a pressure of 45 tsi (620.5 MPa) to the mixture using a press. The spectra were obtained with 4 cm^{-1} resolution and 64 scans.

2.7. Thermo gravimetrical analysis

Thermogravimetric analyses (TGA) were performed using an SDT Q600 V 8.0 instrument (TA Instruments). The system was pre-equilibrated at 30 °C, then a ramp from 30 to 900 °C with a 10 °C min^{-1} heating rate was performed under nitrogen flow. Before the measure the materials were ground with mortar and pestle and the measurement was performed on 20 mg of each sample. The temperature range considered to estimate the organic material content was between 150 °C and 500 °C.

2.8. Scanning electron microscopy observation

All SEM images were acquired using a ZEISS Leo 1530 Gemini field emission scanning electron microscope (SEM) operating at 5 kV. All samples were dried under vacuum in a desiccator and gold-coated (about 10 nm) before their observation.

2.9. BET

The specific surface area of the samples was measured by the multiple BET method using a Gemini VII 2390 Series Surface Area Analyzer (Micromeritics Instrument Corporation) with a nitrogen flow. Each sample was dispersed in isopropanol in order to perform the measurement.

2.10. Dye adsorption kinetics experiments

Adsorption kinetics experiments were carried out suspending 25 mg of each material in 5 mL of dye in a 50 mM pH 7.2 bis-tris buffer solution. The suspensions were kept in a 15 mL polypropylene conical centrifuge tubes at room temperature under mechanical stirring. Two dyes were tested that are Blue Methylene and Eosin Y both having an absorption maximum in the visible region (668 nm and 517 nm, respectively). The dye concentration in solution was measured by a UV-Vis spectrophotometer (Cary 300 Bio, Agilent Technologies) and the amount of dye adsorbed q_t (mg g^{-1}) at the time t (min) was calculated using the following the Eq. (1):

$$q_t = \frac{(C_0 - C_t)V}{m} \quad (1)$$

where C_0 (mg L^{-1}) is the initial dye concentration, C_t (mg L^{-1}) is the dye concentration at time t, V (L) is the volume of the dye solution and m (g) is the mass of the substrate.

For each measurement, the dye solution was centrifuged at 10,000 rpm for 90 s and the supernatant transferred into a plastic cuvette with 1 cm optical path. The spectra were recorded after 30 min, 1 h, 2 h, 4 h and 24 h using a spectral range of 450–800 nm.

2.10.1. Dye adsorption isotherm experiments

Adsorption isotherm experiments were carried out using the same procedure of the adsorption kinetics experiments. Different dye concentrations were tested that are 0.005, 0.0075, 0.01, 0.025 and 0.05 mM. Three isotherm models were tested i. e. the Langmuir isotherm (Eq. (2)), the Freundlich isotherm (Eq. (3)) and the Dubinin-Radushkevich isotherm (Eq. (4)):

$$\frac{1}{q_e} = \frac{1}{Q_{MAX} K_L C_e} + \frac{1}{Q_{MAX}} \quad (2)$$

$$\log q_e = \log K_F + \frac{1}{n} \log C_e \quad (3)$$

$$\ln q_e = \ln Q_{MAX} - K_D \varepsilon^2 \quad (4)$$

Where q_e (mg g^{-1}) is the amount of dye adsorbed at equilibrium, Q_{MAX} (mg g^{-1}) is the maximum adsorption capacity from the adsorption models, C_e (mg L^{-1}) is the concentration of the adsorbate at equilibrium, K_L (mg^{-1}) is the Langmuir constant, n is a constant representing the favorable degree of adsorption, K_F (mg g^{-1}) is the Freundlich constant, K_D (mol^2 kJ^{-2}) is the Dubinin-Radushkevich constant and ε (J mol^{-1}) is the Polanyi potential calculated as follows:

$$\varepsilon = RT \ln\left(1 + \frac{1}{C_e}\right) \quad (5)$$

Where R (J mol^{-1} K^{-1}) is the gas constant and T (K) is the experimental temperature.

3. Results and discussion

3.1. Material's properties

An initial characterization of shell fragments from the two species, BS and CMC, was performed after washing with deionized water and drying in an oven overnight at 50 °C (Fig. S1A and B). The analyses of the X-ray diffraction patterns and the FTIR spectra (Fig. 1) revealed the presence of proteins and crystalline material made of α-chitin and calcite in the carapaces of both species. This was indicated by the occurrence of the characteristic diffraction peaks (020) and (110) of α-chitin at 2theta angles of 9 and 19 °, respectively, while calcite appeared from the diffraction peaks (012), (104), and (013) at 23, 29, and 39 ° respectively. The vibrational adsorption bands due to chitin and proteins at 3400 cm^{-1}, 3100 cm^{-1} and 1700 cm^{-1} corresponding to the O-H stretching, aliphatic compound and the CH_3 stretching, and amide I stretching of C═O group, respectively, and to calcite at 1800 cm^{-1}, 1410 cm^{-1}, 875 cm^{-1} and 712 cm^{-1}, were detected. In addition to these signals, in BS shells but not in CMC shells, the diffraction pattern showed diffraction peaks at 2theta value of 27, 33 and 44 ° and the FTIR spectrum adsorption band at 744 cm^{-1}, both of which indicating the presence of vaterite. This phase represented the 45 wt% of crystalline minerals in BS shells.

Vaterite has been found to form in shrimp shells during frozen storage, specifically in the pink shrimp, *Pandalus borealis*. The white spots, made of calcite and vaterite, increase in size and eventually cover the entire shell, which was originally transparent. It has been suggested that α-chitin is crucial in the crystallization process of these white spots, as it is a key component of their composition [30]. Vaterite has been reported to form at relatively low temperatures in wet conditions from amorphous calcium carbonate (ACC) [31], suggesting that vaterite formed from ACC in BS.

No vaterite formation was found in CMC shells, indicating that there may not be significant amounts of ACC present in the original material.

The shells' organic material content was evaluated using thermo-gravimetrical analysis (TGA). The analyses of the thermal profiles (Fig. S2) revealed that BS shells have a higher content of water and organic material (61.46 wt%) than the CMC ones (47.50 wt%). The relative content of proteins and chitin was not estimated at this stage.

After characterizing the raw material, different chemical treatments were performed: (i) deproteinization using a reflux reaction with 1 M sodium hydroxide solution at 100 °C; (ii) bleaching using a 5 % v/v sodium hypochlorite solution for 8 days to remove organic material, such as proteins, chitin and lipids; (iii) bleaching followed by thermal treatment in the oven at 220 °C for 48 h to also remove intra-crystalline organic material; (iv) demineralization using hydrochloric acid to dissolve $CaCO_3$, followed by deproteinization to extract chitin from the shells [32].

An interesting finding from the analysis of the materials extracted from the BS shells was the detection of vaterite following the deproteinization process and the application of heat. This was evidenced by the appearance of distinct peaks in the X-ray diffraction patterns (Fig. 2C), which supports our earlier observation from the FTIR analysis of the unprocessed material. This supports the previous finding that vaterite is stabilized by α-chitin [30,33].

The FTIR spectra analysis revealed a decrease in protein content in both shell types following alkaline and bleaching treatments, as evidenced by the disappearance of the band at approximately 1600 cm^{-1} corresponding to the N-H bending of the peptide group and an increase in the relative intensities of the vibrational bands associated with $CaCO_3$ (Fig. 2B and D). Additionally, thermo-gravimetrical analysis indicated a decrease in the weight loss associated with the pyrolysis of the organic material after these treatments (Fig. S3 and S4).

After alkaline treatment the remaining material was 32.76 wt% for shrimp and 21.09 wt% for crab (Table 1), indicating that in the BS shells there is about 29 wt% of proteic material, while in the CMC ones it is

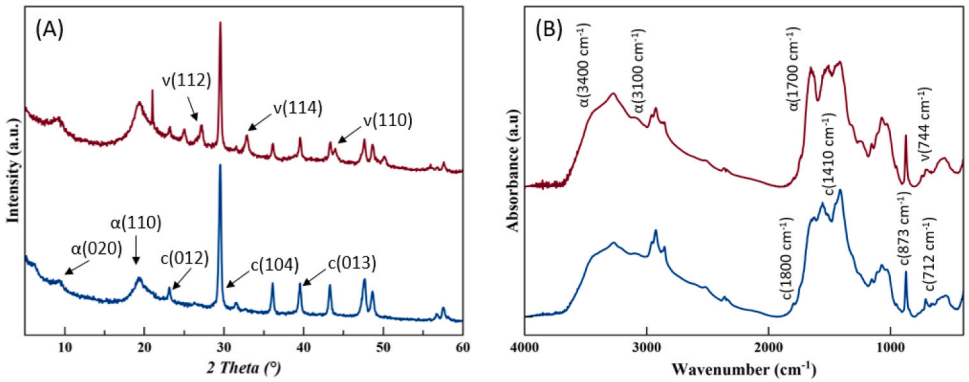

Fig. 1. X-ray powder diffraction patterns (A) and FTIR spectra (B) of CMC (blue) and BS (red) waste shells. The diffraction patterns were indexed accordingly to the PDF 00–005–0586 for calcite, PDF 00–024–0030 for vaterite and PDF 00–035–1974 for α-chitin.

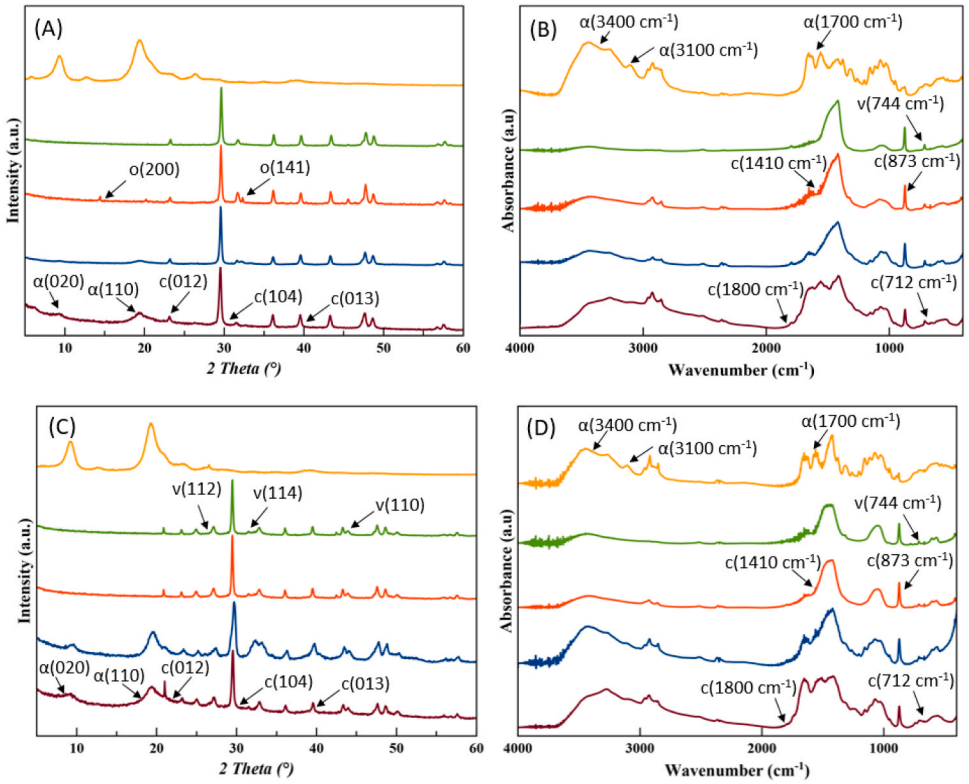

Fig. 2. X-ray powder diffraction patterns and FTIR spectra of CMC (A, B) and BS (C, D), respectively, raw material (red), deproteinized (blue), bleached (orange) and bleached/heated (green) one, and chitin (yellow). The diffraction patterns were indexed accordingly to the PDF 00–005–0586 for calcite, PDF 00–024–0030 for vaterite, PDF 00–035–1974 for α-chitin and PDF 01–087–0655 for calcium oxalate.

about 26 wt%. After the bleaching treatment, the weight loss was 9.56 wt% for the shrimp and 9.32 wt% for the crab. After the bleaching and thermal processes, the organic material content was lower than in the only bleached sample and it was 4.73 wt% for the shrimp and 3.49 wt% for the crab. These results indicated that chitin was not totally removed in the bleached and the bleached/heated materials, as was also indicated by the vibrational bands from chitin observed in the FTIR spectra (Fig. 2B and D). The X-ray diffraction pattern data, however, did not reveal any peak linked to α-chitin, indicating that it may be present in the sample in a quantity too low to be detected by X-ray diffraction or in an amorphous state. Additionally, in the bleached crab diffraction pattern (Fig. 2A), additional diffraction peaks at approximately 14 and 32 °, which are linked to calcium oxalate, were observed. This is a by-product resulting from the chitin oxidation reaction [34].

In the last step, after the demineralization and deproteinization processes, only the peaks relatives to α-chitin were present in the diffraction patterns, confirming that $CaCO_3$ had been completely removed (Fig. 2A e C). The weight loss associated to the organic material in both species increased and it was 79.98 wt% for shrimp and 73.91 wt % for crab, in agreement with the removal of $CaCO_3$ (Table 1).

The BET technique was used to investigate the specific surface area of the material. This method involves creating a N_2 monolayer on the surface of the sample being studied. This can be challenging to accomplish when the material has a complex morphology and mixed surface chemistry due to its inorganic/organic hybrid composition and high chitin content [35]. For these reasons, it is challenging to explain the specific surface area obtained from the BET measurements (Table 1). Nevertheless, they can be valuable for comparing samples that underwent the same treatment. The samples after bleaching and after bleaching/heating processes have a similar amount of organic material,

Table 1
Main shellfish components (prot. = proteins; chit. = chitin; $CaCO_3$ = calcium carbonate), mineral phase and specific surface area (SSA) of CMC and BS raw material (A) and deproteinized (B), bleached (C), bleached/heated (D) ones, and chitin (E).

Sample	Main components	Crab			Shrimp		
		Mass (wt%)	**Mineral Phase**[b]	**SSA** ($m^2\ g^{-1}$)	**Mass** (wt%)	**Mineral Phase**	**SSA** ($m^2\ g^{-1}$)
A	prot.	26.41	cal.[c]	ND[a]	28.70	cal. (55.60 wt%)	ND[a]
	chit.	21.09			32.76	vat.[e] (44.40 wt%)	
	$CaCO_3$	52.50			38.54		
B	chit.	21.09	cal.	27.64	32.76	calc. (65.70 wt%)	11.24
	$CaCO_3$	78.91			67.24	vat. (34.30 wt%)	
C	chit.	9.32	cal. (97.61 wt%)	12.71	9.56	calc. (55.91 wt%)	20.22
	$CaCO_3$	90.68	CaOx. (2.39 wt%)[d]		90.44	vat. (44.09 wt%)	
D	chit.	3.49	cal.	27.93	4.73	cal (56.32 wt%)	48.97
	$CaCO_3$	96.51			95.27	vat (43.68 wt%)	
E	chit.	100	-	ND[a]	100	-	ND[a]

[a] an accurate determination of the specific surface area was not possible.
[b] When not indicated the wt% only one mineral phase is present.
[c] cal. indicates calcite.
[d] CaOx indicates calcium oxalate.
[e] vat. Indicates vaterite.

with the remaining being calcium carbonate. In this instance, the surface area of the shrimp sample is greater than that of the crab. This difference may be linked to the presence of vaterite in the shrimp-derived material, which has a higher surface area than calcite for particles having similar size [36].

The surface area of the chitin material extracted from shrimps and

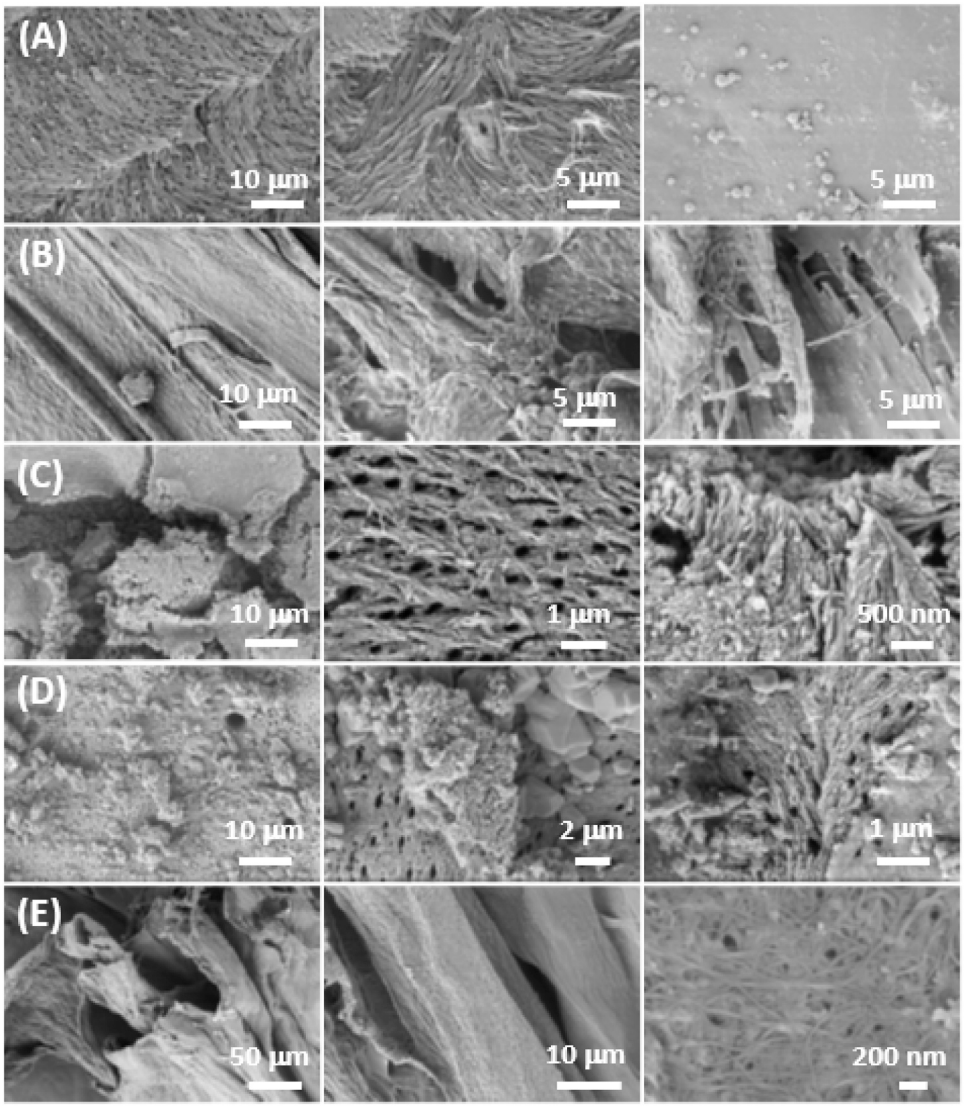

Fig. 3. SEM images of CMC raw material (A) and deproteinized (B), bleached (C), bleached/heated (D) ones, and chitin (E).

crabs has been reported to be about 3 and 3.6 $m^2 g^{-1}$, respectively [37]. However, these substrates showed much higher surface area than the ones here presented, when this was calculated considering the capability to absorb dyes [35,38].

The surface morphology of CMC and BM shells pristine and derived materials was investigated by SEM (Figs. 3 and 4). In a general overview, all the samples were heterogenous and with very complex morphology. The two species show a different texture and organization of the shell fibers and grains, which change after the different chemical-thermal processes. Prior each treatment, the shrimp shell surface (Fig. 4A) shows an ordered fibrous microstructure with chitin fibre embedded in a framework of organic material forming a compact matrix, which is the scaffold where calcium carbonate is located. This structural organization is also observed in the crab pristine cuticle but in this case the organization of chitin fibers result in a porous texture (Fig. 3A). After the deproteinization reaction, the shell structure becomes more disordered and less compact in both species, probably due to the removal of proteins which may act as a fixative for chitin fibers and $CaCO_3$ particles (Figs. 3B and 4B). For the same reason, chitin extracted from both species looks rough and highly exfoliated (Figs. 3E and 4E). After the bleaching processes, the main observable component of the matrix shell is the mineral phase, confirming the reduction of chitin content upon treatments. This is very evident in the crab shell bleached/heated materials where calcite crystals can be observed (Fig. 3D).

SEM observations were also carried out on the different substrates after the adsorption process (refer to the next section). Unfortunately, the complex shapes and morphologies observed posed a challenge in identifying variations associated with the adsorption process.

3.2. Dye adsorption properties

The potential use of all the materials obtained from CMC and BS waste shells was tested in water remediation, in accordance with literature and showing that these low-cost adsorbents have a high capacity for removing specific dyes [39,40] We conducted extensive research to explore the use of raw materials as substrates for adsorbing organic dyes. However, the initial material, obtained from industrial processing, continues to release soluble material even after multiple water washes, likely due to organic degradation. This ongoing release hinders an accurate assessment of the adsorption capacity.

All substrates derived from CMC and BS were examined for their ability to adsorb two common model dyes used in the textile industry: Eosin Y (EY), an anionic dye, and Blue Methylene (BM), a cationic dye. The tests were conducted in a 50 mM pH 7.2 bis-tris buffer solution at a concentration of 0.01 mM, which is both environmentally and industrially significant. The adsorption of both dyes on all the substrates

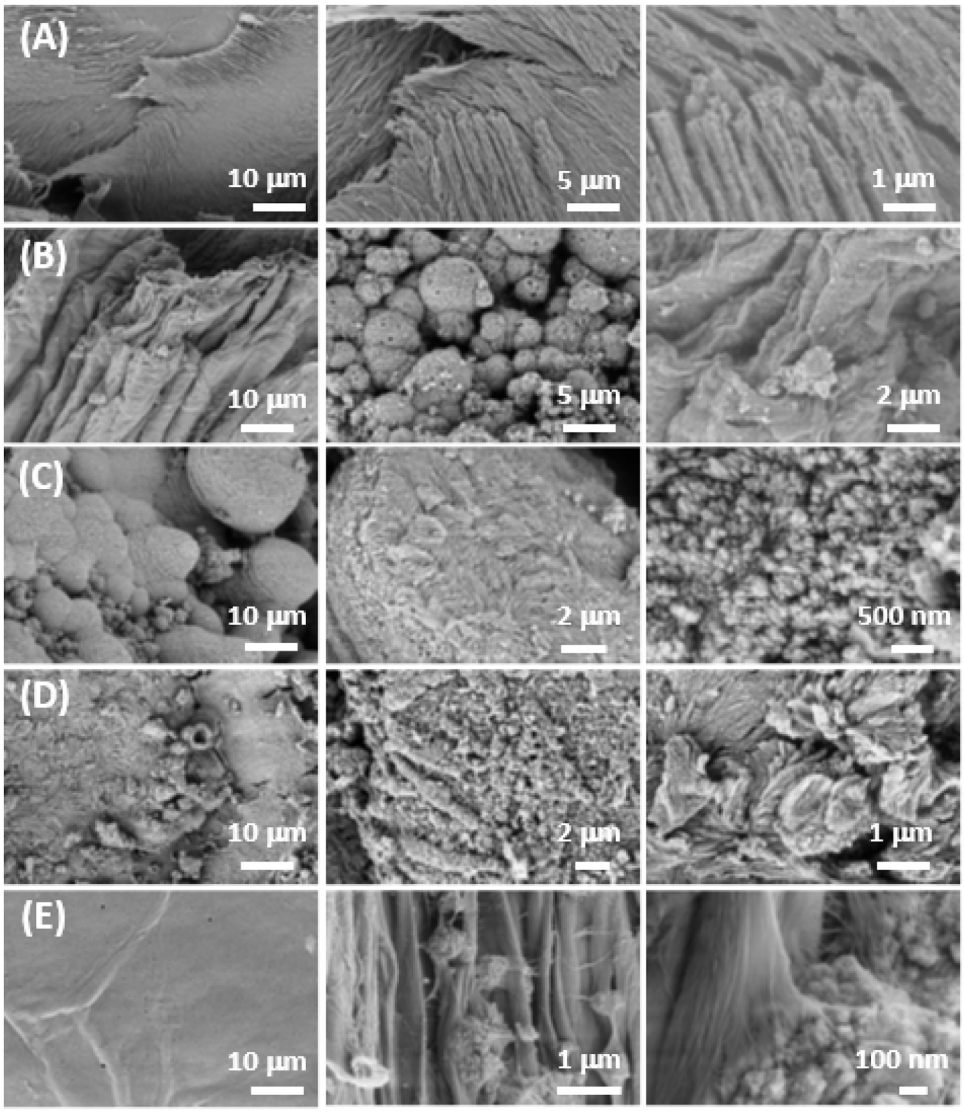

Fig. 4. SEM images of BS raw material (A) and deproteinized (B), bleached (C), bleached/heated (D) ones, and chitin (E).

reached equilibrium within 24 h (Fig. S5). Table 2 summarizes the maximum adsorption capacity of the different materials of both dyes, after adsorption kinetics experiments.

Overall, materials obtained from BS generally exhibited a greater ability to adsorb both dyes compared to those from CMC. The only exception was the bleached/heated material, which had a higher adsorption capacity for BM on CMC, although the amount absorbed was low and near the limit of detection. Notably, all substrates showed a higher adsorption capacity for EY, except for the bleached ones. These findings indicate that the bleached materials undergo a change in surface chemistry after thermal treatment, leading to the replacement of some carbonate groups with hydroxyl groups in the coordination of calcium ions [41]. When adsorbing BM and EY, the maximum adsorption capacity was exhibited by the shrimp bleached material (0.45 mg g^{-1}) and chitin (0.99 mg g^{-1}), respectively, while the minimum one by the shrimp bleached/heated material (0.081 mg g^{-1}) and the crab bleached/heated ones (0.056 mg g^{-1}), respectively. These results align with the aforementioned considerations on the specific surface of chitin materials and the data reported in Table 1.

To assess the adsorption kinetics mechanism, an analysis of isotherm models was conducted. The experimental data were fitted with: (i) the Langmuir isotherm, which assumes a uniform surface of the substrate and an adsorption mechanism controlled by chemical processes leading to monolayer formation; (ii) the Freundlich isotherm, which assumes a non-uniform surface of the substrates, an adsorption mechanism controlled by physical processes, and the formation of multiple layers; (iii) the Dubinin-Radushkevich isotherm, which is similar to the Freundlich model but takes into account microporous surfaces. [42]. In Tables 3 and 4 the calculated parameters from the best fitting of the adsorption isotherms for the substrates in BM and EY, respectively, are reported.

The adsorption data best fit with a Freundlich isotherm, indicating no site-specific interaction and the formation of multilayers. This result is consistent with the complex morphology of the substrates, which have a heterogeneous surface, as shown by the SEM observations. (Figs. 3 and 4).

When discussing the experimental data of this study, it is important to consider the complexity of the system and the criterion adopted in the research, which aimed to utilize all components of the waste material. This objective was successfully achieved. While the adsorption capacity of the material is lower compared to commonly used materials,[43] it is in line with similar materials [44]. It is worth noting that the material did not undergo any chemical functionalization to enhance its adsorption capacity, setting it apart from other studies on different substrates. For instance, clay has been modified chemically and physically to improve its adsorption capacity [45–47]. The chemical nature and site-specific adsorption mechanism allowed for a simulation of the absorption process on such a substrate [48], which was not possible in the system studied here where adsorption is not site-specific. However, this does not diminish the significance of the work in demonstrating that all components of a waste material can be utilized for the diverse adsorption of organic dyes.

Table 2
Maximum adsorption capacity (q_{MAX}) from the adsorption kinetics experiments of CMC and BS deproteinized (A), bleached (B), bleached/heated (C) shells, and chitin (D) in Blue Methylene (BM) and Eosin Y (EY) 0.01 mM solutions at pH 7.2. The dye adsorbed is reported as the mass of dye (mg) over the mass of substrate (g).

Sample	Crab		Shrimp	
	q_{MAX} BM (mg g^{-1})	q_{MAX} EY (mg g^{-1})	q_{MAX} BM (mg g^{-1})	q_{MAX} EY (mg g^{-1})
A	0.12 ± 0.01	0.19 ± 0.02	0.203 ± 0.003	0.29 ± 0.02
B	0.372 ± 0.001	0.09 ± 0.01	0.454 ± 0.009	0.25 ± 0.03
C	0.0985 ± 0.0007	0.0557 ± 0.0003	0.0809 ± 0.0002	0.0821 ± 0.0006
D	0.26 ± 0.02	0.641 ± 0.005	0.310 ± 0.005	0.99 ± 0.07

Table 3
Calculated parameters from the best fitting of the adsorption isotherms with different models of CMC and BS deproteinized (A, B), bleached (C, D), bleached/heated (E, F) shells, and chitin (G, H) in Blue Methylene.

Sample	Model	R^2	n	K[a]	Q_{MAX} (mg g^{-1})
A	Freundlich	0.9934	1.0305	0.0545	/
B	Freundlich	0.9729	1.1050	0.0770	/
C	Dub. - Radush.	0.9193	/	1.4329	0.5430
D	Freundlich	0.9799	1.2054	0.1337	/
E	Freundlich	0.863	3.1387	0.04151	/
F	Freundlich	0.9318	2.6954	0.0458	/
G	Freundlich	0.9484	1.0113	0.0494	/
H	Freundlich	0.9988	0.9505	0.0851	/

[a] The unit of measure for the parameter K is mg^{-1} for the Langmuir model, mg g^{-1} for the Freundlich and mol^2 kJ^{-2} for the Dubinin-Radushkevich one.

Table 4
Calculated parameters from the best fitting of the adsorption isotherms with different models of CMC and BS deproteinized (A, B), bleached (C, D), bleached/heated (E, F) shells, and chitin (G, H) in Eosin Y.

Sample	Model	R^2	n	K[a]	Q_{MAX} (mg g^{-1})
A	Freundlich	0.9631	0.9281	0.0245	/
B	Freundlich	0.913	1.0825	0.0591	/
C	Langmuir	0.9129	/	0.0618	0.2750
D	Langmuir	0.6308	/	0.1330	0.2975
E	Freundlich	0.9535	0.9265	0.0085	/
F	Freundlich	0.9524	0.9366	0.0114	/
G	Freundlich	0.9679	0.9800	0.0293	/
H	Freundlich	0.9342	1.2992	0.1531	/

[a] The unit of measure for the parameter K is mg^{-1} for the Langmuir model, mg g^{-1} for the Freundlich and mol^2 kJ^{-2} for the Dubinin-Radushkevich one.

4. Conclusions

This work has shown that it is possible to obtain multifunctional materials with different characteristics, such as composition, shape, and morphology, from shrimp and crab shells. Our approach is innovative because we demonstrate the sequential study of the various processes that allows for the isolation of the components of the shells, whose characteristics depend on the species. As a case study, among the many applications of chitin and calcium carbonate, we decided to evaluate the ability of the different substrates to act as absorbent agents for dyes from polluted waters, which is relevant in an industrial area. The results show that materials obtained from shrimp shells have a higher absorbent capacity than those obtained from crab shells. It is important to highlight that the processes adopted to obtain the various materials can be scaled on an industrial level, offering a long-term vision for the application of this experimental strategy for the development of technology for the treatment of these residual bioresources.

Funding sources

This research was supported by ERA-NET Cofund on Blue Bioeconomy (BlueBio) projects CASEAWA (grant number: 817992) and BlueCC (grant number: 02362).

Author contributions

The manuscript was written through the contributions of all authors. All authors have given approval to the final version of the manuscript.

CRediT authorship contribution statement

C. Triunfo: Writing – review & editing, Formal analysis, Data

curation. **K. Tsirtsidou:** Writing – review & editing, Validation, Formal analysis, Data curation. **K. Vanhoutte:** Writing – review & editing, Validation, Formal analysis, Data curation. **A. Mucaria:** Writing – review & editing, Formal analysis, Data curation. **D. Montroni:** Writing – review & editing, Validation, Formal analysis, Data curation. **S. Fermani:** Writing – review & editing, Funding acquisition, Formal analysis, Data curation. **G. Falini:** Writing – review & editing, Writing – original draft, Validation, Funding acquisition, Conceptualization. **J. Robbens:** Writing – review & editing, Validation, Supervision, Funding acquisition, Conceptualization.

Declaration of Competing Interest

The authors declare that they have no known competing financial interests or personal relationships that could have appeared to influence the work reported in this paper.

Data Availability

Data will be made available on request.

Appendix A. Supporting information

Supplementary data associated with this article can be found in the online version at doi:10.1016/j.mtcomm.2024.109441.

References

[1] N. Yan, X. Chen, Sustainability: don't waste seafood waste, Nature 524 (2015) 155–157.
[2] J.P. Morris, T. Backeljau, G. Chapelle, Shells from aquaculture: a valuable biomaterial, not a nuisance waste product, Rev. Aquac. 11 (2019) 42–57.
[3] Y. Zou, M. Heyndrickx, J. Debode, K. Raes, D. de Pascale, P. Behan, M. Giltrap, C. O'Connor, R.G. Solstad, K. Lian, T. Altintzoglou, R. Dragoy, N. Scheers, I. Underland, J. Robbens, Valorisation of crustacean and bivalve processing side streams for industrial fast time-to-market products: a review from the European Union regulation perspective, Front. Mar. Sci. 10 (2023) 1068151.
[4] N. Topić Popović, V. Lorencin, I. Strunjak-Perović, R. Čož-Rakovac, Shell waste management and utilization: mitigating organic pollution and enhancing sustainability, Appl. Sci. 13 (2023).
[5] Y. Zou, J. Robbens, M. Heyndrickx, J. Debode, K. Raes, Bioprocessing of marine crustacean side-streams into bioactives: a review, J. Chem. Technol. Biotechnol. 96 (2021) 1465–1474.
[6] A. da S. Cardoso, E.R.K. Rabbani, T.D. Delmiro, J.F.B. Mocock, S.P.R. da Silva, G. Filippelli, J.V. da S. Macedo, E.C.B. Monteiro, Mollusk shell waste: alternatives for reuse in construction, Int. J. Environ. Waste Manag. 31 (2023) 61–80.
[7] H. Nagasawa, The crustacean cuticle: structure, composition and mineralization, Front. Biosci. (Elite Ed.). 4 (2012) 711–720, https://doi.org/10.2741/E412.
[8] Y. Kato, H. Onishi, Y. Machida, Application of chitin and chitosan derivatives in the pharmaceutical field, Curr. Pharm. Biotechnol. 4 (2003) 303–309.
[9] I. Aranaz, N. Acosta, C. Civera, B. Elorza, J. Mingo, C. Castro, M.D.L.L. Gandía, A. Heras Caballero, Cosmetics and cosmeceutical applications of chitin, chitosan and their derivatives, Polymers (Basel) 10 (2018) 213.
[10] S. Peter, N. Lyczko, D. Gopakumar, H.J. Maria, A. Nzihou, S. Thomas, Chitin and chitosan based composites for energy and environmental applications: a review, Waste Biomass Valoriz. 12 (2021) 4777–4804.
[11] Y.-Q. Niu, J.-H. Liu, C. Aymonier, S. Fermani, D. Kralj, G. Falini, C.-H. Zhou, Calcium carbonate: controlled synthesis, surface functionalization, and nanostructured materials, Chem. Soc. Rev. 51 (2022) 7883–7943.
[12] S.J. Sreeja, K. Tamilarutselvi, A. Tamilselvi, K.P. Sarojini, K.J. Jasmin, M. M. Malini, Production of chitin and conversion into chitosan from crab (Scylla tranquebarica) shells and evaluation of its antioxidant activities, Biomass Convers. Biorefinery (2023).
[13] P. Ambigaipalan, F. Shahidi, Bioactive peptides from shrimp shell processing discards: antioxidant and biological activities, J. Funct. Foods 34 (2017) 7–17.
[14] G.M. Mathew, D.C. Mathew, R.K. Sukumaran, R. Sindhu, C.-C. Huang, P. Binod, R. Sirohi, S.-H. Kim, A. Pandey, Sustainable and eco-friendly strategies for shrimp shell valorization, Environ. Pollut. 267 (2020) 115656.
[15] A. Miron, A. Sarbu, A. Zaharia, T. Sandu, H. Iovu, R.C. Fierascu, A.-L. Neagu, A.-L. Chiriac, T.-V. Iordache, A top-down procedure for synthesizing calcium carbonate-enriched chitosan from shrimp shell wastes, Gels 8 (2022) 742.
[16] D.S. Kim, Pb2+ removal from aqueous solution using crab shell treated by acid and alkali, Bioresour. Technol. 94 (2004) 345–348, https://doi.org/10.1016/j.biortech.2003.10.030.
[17] I. Anastopoulos, A. Bhatnagar, D.N. Bikiaris, G.Z. Kyzas, Chitin adsorbents for toxic metals: a review, Int. J. Mol. Sci. 18 (2017) 114.
[18] J. Wang, C. Chen, Chitosan-based biosorbents: modification and application for biosorption of heavy metals and radionuclides, Bioresour. Technol. 160 (2014) 129–141.
[19] D.J. Jeon, S.H. Yeom, Recycling wasted biomaterial, crab shells, as an adsorbent for the removal of high concentration of phosphate, Bioresour. Technol. 100 (2009) 2646–2649.
[20] M.J. Ahmed, B.H. Hameed, E.H. Hummadi, Review on recent progress in chitosan/chitin-carbonaceous material composites for the adsorption of water pollutants, Carbohydr. Polym. 247 (2020) 116690.
[21] M.A. Robinson-Lora, R.A. Brennan, The use of crab-shell chitin for biological denitrification: batch and column tests, Bioresour. Technol. 100 (2009) 534–541.
[22] P. Sirajudheen, N.C. Poovathumkuzhi, S. Vigneshwaran, B.M. Chelaveettil, S. Meenakshi, Applications of chitin and chitosan based biomaterials for the adsorptive removal of textile dyes from water — a comprehensive review, Carbohydr. Polym. 273 (2021) 118604.
[23] H. Ighnih, R. Haounati, H. Ouachtak, A. Regti, B. El Ibrahimi, N. Hafid, A. Jada, M. L. Taha, A.A. Addi, Efficient removal of hazardous dye from aqueous solutions using magnetic kaolinite nanocomposite: experimental and Monte Carlo simulation studies, Inorg. Chem. Commun. 153 (2023) 110886.
[24] F. Largo, R. Haounati, H. Ouachtak, N. Hafid, A. Jada, A.A. Addi, Design of organically modified sepiolite and its use as adsorbent for hazardous Malachite Green dye removal from water, Water Air Soil Pollut. 234 (2023) 183.
[25] W.F. Sye, L.C. Lu, J.W. Tai, C.I. Wang, Applications of chitosan beads and porous crab shell powder combined with solid-phase microextraction for detection and the removal of colour from textile wastewater, Carbohydr. Polym. 72 (2008) 550–556.
[26] M. Geetha Devi, J.J. Dumaran, S. Feroz, Dairy wastewater treatment using low molecular weight crab shell chitosan, J. Inst. Eng. Ser. E 93 (2012) 9–14.
[27] L. Dai, W. Zhu, L. He, F. Tan, N. Zhu, Q. Zhou, M. He, G. Hu, Calcium-rich biochar from crab shell: an unexpected super adsorbent for dye removal, Bioresour. Technol. 267 (2018) 510–516.
[28] M. Meriatna, S.M. Utari, R. Mulyawan, M. Muhammad, Z. Zulmiardi, Methyl orange absorption using chitosan from shrimp skin as an adsorbent, Int. J. Eng. Sci. Inf. Technol. 3 (2023) 25–30.
[29] C. Triunfo, S. Gartner, C. Marchini, S. Fermani, G. Maoloni, S. Goffredo, J. Gomez Morales, H. Cölfen, G. Falini, Recovering and exploiting aragonite and calcite single crystals with biologically controlled shapes from mussel shells, ACS Omega 7 (2022) 43992–43999.
[30] A. Mikkelsen, S.B. Engelsen, H.C.B. Hansen, O. Larsen, L.H. Skibsted, Calcium carbonate crystallization in the α-chitin matrix of the shell of pink shrimp, Pandalus borealis, during frozen storage, J. Cryst. Growth 177 (1997) 125–134.
[31] T. Ogino, T. Suzuki, K. Sawada, The formation and transformation mechanism of calcium carbonate in water, Geochim. Cosmochim. Acta 51 (1987) 2757–2767.
[32] B. Vandecasteele, F. Amery, S. Ommeslag, K. Vanhoutte, R. Visser, J. Robbens, C. De Tender, J. Debode, Chemically versus thermally processed brown shrimp shells or Chinese mitten crab as a source of chitin, nutrients or salts and as microbial stimulant in soilless strawberry cultivation, Sci. Total Environ. 771 (2021) 145263.
[33] G. Falini, S. Fermani, A. Ripamonti, Crystallization of calcium carbonate salts into beta-chitin scaffold, J. Inorg. Biochem. 91 (2002) 475–480.
[34] M.F. Queiroz, K.R.T. Melo, D.A. Sabry, G.L. Sassaki, H.A.O. Rocha, L.S. Costa, Gallic acid-chitosan conjugate inhibits the formation of calcium oxalate crystals, Molecules 24 (2019) 2074.
[35] G. Akkaya, I. Uzun, F. Güzel, Kinetics of the adsorption of reactive dyes by chitin, Dye. Pigment. 73 (2007) 168–177.
[36] R. Sasamoto, Y. Kanda, S. Yamanaka, CaCO3 vaterite microparticles for biomedical and personal care applications, Chemosphere 297 (2022) 134057, https://doi.org/10.1016/j.chemosphere.2022.134057.
[37] N. Jaafarzadeh, N. Mengelizadeh, A. Takdastan, M. Heidari-Farsani, N. Niknam, Adsorption of Zn (II) from aqueous solution by using chitin extraction from crustaceous shell, J. Adv. Environ. Heal. Res. 2 (2014) 110–119.
[38] M. Fabbricino, L. Pontoni, Use of non-treated shrimp-shells for textile dye removal from wastewater, J. Environ. Chem. Eng. 4 (2016) 4100–4106.
[39] G. Crini, Non-conventional low-cost adsorbents for dye removal: a review, Bioresour. Technol. 97 (2006) 1061–1085.
[40] M. Fomina, G.M. Gadd, Biosorption: current perspectives on concept, definition and application, Bioresour. Technol. 160 (2014) 3–14.
[41] M. Ban, T. Luxbacher, J. Lützenkirchen, A. Viani, S. Bianchi, K. Hradil, A. Rohatsch, V. Castelvetro, Evolution of calcite surfaces upon thermal decomposition, characterized by electrokinetics, in-situ XRD, and SEM, Colloids Surf. A Physicochem. Eng. Asp. 624 (2021) 126761.
[42] M.M. Majd, V. Kordzadeh-Kermani, V. Ghalandari, A. Askari, M. Sillanpää, Adsorption isotherm models: a comprehensive and systematic review (2010–2020), Sci. Total Environ. 812 (2022) 151334.
[43] S. Babel, T.A. Kurniawan, Low-cost adsorbents for heavy metals uptake from contaminated water: a review, J. Hazard. Mater. 97 (2003) 219–243, https://doi.org/10.1016/S0304-3894(02)00263-7.
[44] D. Montroni, C. Piccinetti, S. Fermani, M. Calvaresi, M.J. Harrington, G. Falini, Exploitation of mussel byssus mariculture waste as a water remediation material, RSC Adv. 7 (2017) 36605–36611, https://doi.org/10.1039/c7ra06664c.
[45] H. Ouachtak, A. El Guerdaoui, R. Haounati, S. Akhouairi, R. El Haouti, N. Hafid, A. A. Addi, B. Šljukić, D.M.F. Santos, M.L. Taha, Highly efficient and fast batch adsorption of orange G dye from polluted water using superb organo-montmorillonite: experimental study and molecular dynamics investigation, J. Mol. Liq. 335 (2021) 116560.
[46] H. Ouachtak, A. El Guerdaoui, R. El Haouti, R. Haounati, H. Ighnih, Y. Toubi, F. Alakhras, R. Rehman, N. Hafid, A.A. Addi, M.L. Taha, Combined molecular

dynamics simulations and experimental studies of the removal of cationic dyes on the eco-friendly adsorbent of activated carbon decorated montmorillonite Mt@AC, RSC Adv. 13 (2023) 5027–5044.

[47] H. Ouachtak, R. El Haouti, A. El Guerdaoui, R. Haounati, E. Amaterz, A.A. Addi, F. Akbal, M.L. Taha, Experimental and molecular dynamics simulation study on the adsorption of Rhodamine B dye on magnetic montmorillonite composite γ-Fe_2O_3@Mt, J. Mol. Liq. 309 (2020) 113142.

[48] R. El Haouti, H. Ouachtak, A. El Guerdaoui, A. Amedlous, E. Amaterz, R. Haounati, A.A. Addi, F. Akbal, N. El Alem, M.L. Taha, Cationic dyes adsorption by Na-montmorillonite nano clay: experimental study combined with a theoretical investigation using DFT-based descriptors and molecular dynamics simulations, J. Mol. Liq. 290 (2019) 111139.